

Supporting Information

Interdigitated Pt-Br chains with π -stacking: an approach toward Robin-Day class I mixed valency in MX-chain complexes

Unjila Afrin,^a Kentaro Fuku,^a Mengxing Cui,^a Hiroaki Iguchi,^{*a} Mohammad Rasel Mian,^a Ryo Nakanishi,^a Shinya Takaishi,^a and Masahiro Yamashita^{*a,b}

^aDepartment of Chemistry, Graduate School of Science, Tohoku University, 6-3 Aramaki-Aza-Aoba, Aoba-ku, Sendai, Miyagi 980-8578, Japan.

^bSchool of Materials Science and Engineering, Nankai University, Tianjin 300350, China.

Table of Contents

Experimental details.....	S2
Crystallographic parameters of 3 (Table S1).....	S3
Relationship between M–X–M distance and M ^{II/IV} –X distance (Figure S1).....	S4
Relationship between M–X–M distance and distortion parameter (<i>d</i>) (Figure S2)....	S5
References.....	S6

Experimental details

Single-crystal X-ray structure determination: Single-crystal X-ray diffraction data of **3** were collected on a Bruker APEX-II diffractometer with a APEX II CCD detector and JAPAN thermal Engineering Co., Ltd Cryo system DX-CS190LD. The crystal structures were solved by using direct methods (SHELXT^{S1}), followed by Fourier syntheses. Structure refinement was performed by using full matrix least-squares procedures using SHELXL^{S2} on F^2 in the Yadokari-XG2009 software.^{S3} CCDC-2083871 contains the supplementary crystallographic data for **3**. These data can be obtained free of charge from the Cambridge Crystallographic Data Centre.

Raman spectroscopy: Room-temperature polarized Raman spectra were acquired on HORIBA LabRAM HR-800 with an YAG laser (532 nm), He–Ne laser (632.8 nm) and an optical microscope.

Ultraviolet-visible absorption spectroscopy: Ultraviolet-visible (UV-Vis) absorption spectra were performed with a JASCO V-670 instrument at room temperature. **1**, **2** and **3** was ground with KBr and compress as pellet before the measurement. The solid-state diffuse reflectance spectrum of **5** dispersed in BaSO₄ was already reported in the previous work.^{S4} The obtained spectrum was transformed to the Kubelka–Munk function, which corresponds to the absorption coefficient, for comparison with the spectra of **1–3**.

Elemental Analysis: Elemental analysis was performed at the Research and Analytical Centre for Giant Molecules, Tohoku University.

Synthesis of [Pt(amp)₂Br](H₂PO₄)₂(3)

[Pt(amp)₂]Br₂ (**1**) was synthesized according to the previous report.^{S4} Then, 11.6 mg (0.0203 mmol) of **1** was added to 1.4 mL of ethanol/water (2:5, v/v) solution, followed by adding 71 mg (0.59 mmol) of NaH₂PO₄. A constant current of 10 μ A was applied to the

solution via Pt electrodes. After five days, yellow crystals of **3** were obtained on the anode. (yield: 25% based on Pt). Elemental analysis, Found: C, 20.89; H, 3.02; N, 8.00. Calc. for $C_{12}H_{20}BrN_4O_8P_2Pt$: C, 21.03; H, 2.94; N, 8.18%.

Table S1 Crystallographic parameter of **3**

Empirical formula	$C_{12}H_{20}BrN_4O_8P_2Pt$
Formula weight	685.26
Temperature/K	296
Crystal system	Triclinic
Space group	P-1
$a/\text{\AA}$	6.6978(15)
$b/\text{\AA}$	8.6438(18)
$c/\text{\AA}$	8.8483(19)
$\alpha/^\circ$	85.271(4)
$\beta/^\circ$	86.921(5)
$\gamma/^\circ$	67.163(4)
Volume/ \AA^3	470.37(18)
Z	1
$\rho_{\text{calc}}/\text{gcm}^{-3}$	2.419
μ/mm^{-1}	9.803
$F(000)$	327.0
Crystal size/mm ³	0.20 × 0.17 × 0.03
Radiation	MoK α ($\lambda = 0.71073$)
2 θ range for data collection/°	6.602 to 69.764
Reflections collected	3655
Independent reflections	3655 [$R_{\text{int}} = 0.0158$, $R_{\text{sigma}} = 0.0392$]
Data/restraints/parameters	3655/0/133
Goodness-of-fit on F^2	1.034
Final R indexes [$I \geq 2\sigma(I)$]	$R_1 = 0.0247$, $wR_2 = 0.0564$
Final R indexes [all data]	$R_1 = 0.0254$, $wR_2 = 0.0567$
Largest diff. peak/hole / e \AA^{-3}	1.44/-1.99

Relationship between M–X–M distance and $M^{II/IV}$ –X distance

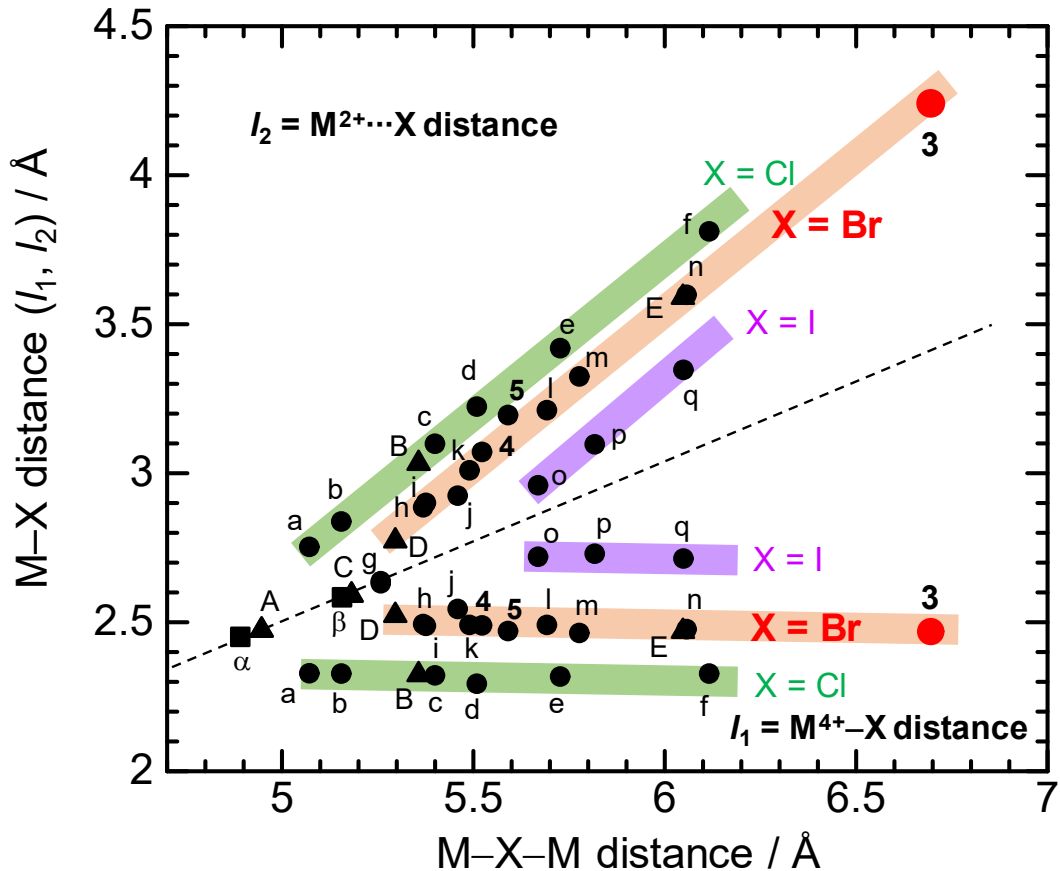


Figure S1. Correlation between M–X–M distance and l_1, l_2 , where l_1 is M^{4+} –X distance and l_2 is $M^{2+}\cdots X$ distance. Square, triangle and circle represent Ni, Pd and Pt-based MX chains, respectively. Red circle represents the target complex **3**. Other data are shown for [Ni(chxn)₂Cl]Cl₂(α),^{S5} [Ni(chxn)₂Br]Br₂(β),^{S5} [Pd(dabdOH)₂Cl]Cl₂(A),^{S6} [Pd(en)₂Cl](ClO₄)₂(B),^{S5} [Pd(dabdOH)₂Br]Br₂(C),^{S7} [Pd(chxn)₂Br]Br₂(D),^{S5} [Pd(en)₂Br](ReO₄)₄(E),^{S8} [Pt(dabdOH)₂Cl]Cl₂(a),^{S9} [Pt(chxn)₂Cl]Cl₂(b),^{S5} [Pt(en)₂Cl](ClO₄)₂(c),^{S5} [Pt(pn)₂Cl](ClO₄)₂(d),^{S10} [Pt(chxn)₂Cl](ClO₄)₂(e),^{S5} [Pt(en)₂Cl](ReO₄)₂(f),^{S8} [Pt(dabdOH)₂Br]Br₂(g),^{S9} [Pt(chxn)₂Br]Br₂(h),^{S5} [Pt(en)₂Br](C₆-Y)₄·H₂O(i),^{S11} [Pt(tn)₂Br](BF₄)₂(j),^{S10} [Pt(en)₂Br](ClO₄)₄ (polymorph I)(k),^{S5} [Pt(en)₂Br](ClO₄)₄ (polymorph II)(l),^{S5} [Pt(chxn)₂Br](ClO₄)₂(m),^{S5} [Pt(en)₂Br](ReO₄)₄(n),^{S8} [Pt(chxn)₂I]₂(o),^{S5} [Pt(en)₂I](ClO₄)₂(p),^{S5} [Pt(en)₂I](ReO₄)₂(q),^{S8} **4** and **5**. Green, orange and purple highlight lines are guides for the eyes for each X⁻ ion. (chxn = cyclohexanediamine; en = ethylenediamine; tn = 1,3-diaminopropane, pn = 1,2-diaminopropane, dabdOH = (2S,3S)-2,3-diaminobutane-1,4-diol.)

Relationship between M–X–M distance and distortion parameter (d)

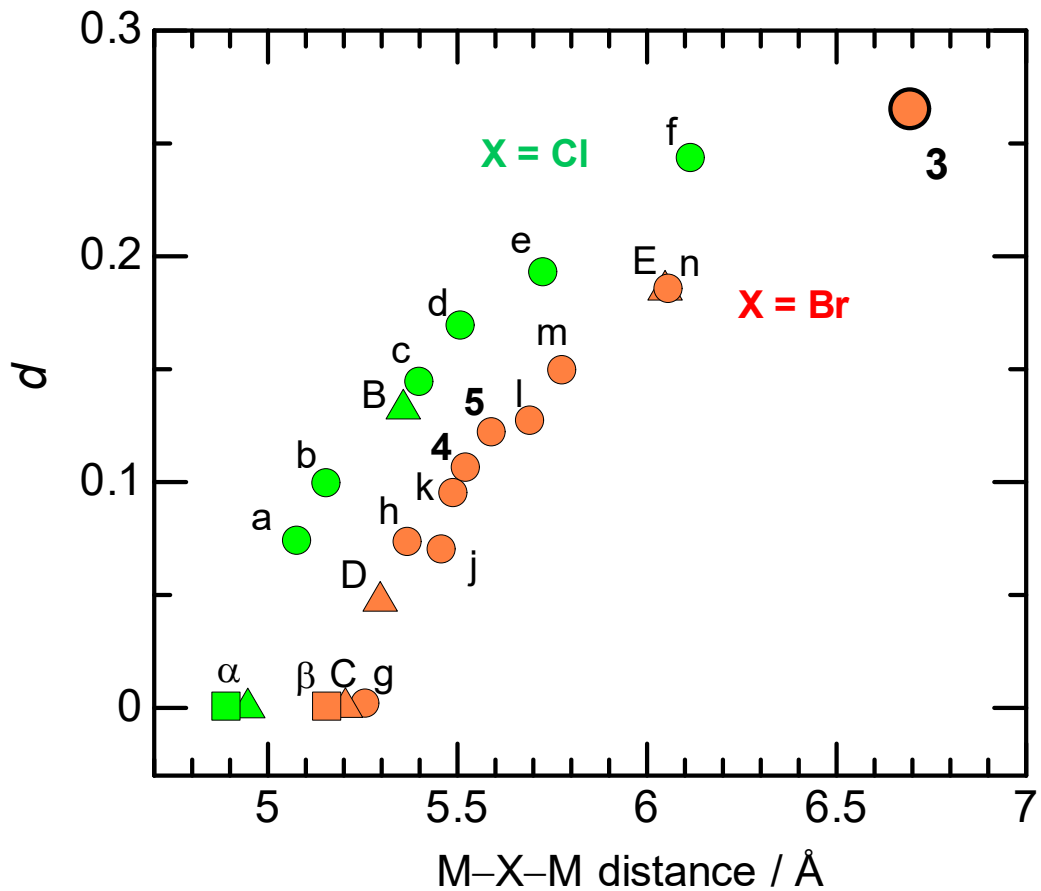


Figure S2. Correlation between M–X–M distance and distortion parameter d , which is defined as $d = (l_2 - l_1)/(\text{Pt–Br–Pt distance})$. Square, triangle and circle represent Ni, Pd and Pt-based MX chains, respectively. Green and orange colour represents Cl- and Br-bridged chains, respectively. The labels are corresponding to those defined in Figure S1.

References:

- (S1) G. M. Sheldrick, *Acta Crystallogr., Sect. A: Found. Adv.*, 2015, **A71**, 3.
- (S2) G. M. Sheldrick, *Acta Crystallogr., Sect. C: Struct. Chem.*, 2015, **C71**, 3.
- (S3) K. Wakita, Yadokari-XG, Software for Crystal Structure Analyses, 2001; Release of Software (Yadokari-XG 2009) for Crystal Structure Analyses; C. Kabuto, S. Akine, T. Nemoto and E. Kwon, *J. Crystallogr. Soc. Jpn.*, 2009, **51**, 218.
- (S4) U. Afrin, H. Iguchi, M. R. Mian, S. Takaishi, H. Yamakawa, T. Terashige, T. Miyamoto, H. Okamoto and M. Yamashita, *Dalton Trans.*, 2019, **48**, 7828.
- (S5) H. Okamoto, M. Yamashita, *Bull. Chem. Soc. Jpn.*, 1998, **71**, 2023.
- (S6) M. R. Mian, M. Wakizaka, T. Yoshida, H. Iguchi, S. Takaishi, U. Afrin, T. Miyamoto, H. Okamoto, H. Tanaka, S. Kuroda, B. K. Breedlove and M. Yamashita, *Dalton Trans.*, 2021, **50**, 1614.
- (S7) M. R. Mian, H. Iguchi, S. Takaishi, H. Murasugi, T. Miyamoto, H. Okamoto, H. Tanaka, S. Kuroda, B. K. Breedlove and M. Yamashita, *J. Am. Chem. Soc.*, 2017, **139**, 6562.
- (S8) S. Kumagai, S. Takaishi, M. Gao, H. Iguchi, B. K. Breedlove and M. Yamashita, *Inorg. Chem.*, 2018, **57**, 3775.
- (S9) M. R. Mian, H. Iguchi, S. Takaishi, U. Afrin, T. Miyamoto, H. Okamoto and M. Yamashita, *Inorg. Chem.*, 2019, **58**, 114.
- (S10) R. J. H. Clark, in *Advances in Infrared and Raman Spectroscopy Volume 11*, ed. R. J. H. Clark and R. E. Hester, Wiley, Hayden, 1984, Chapter 3.
- (S11) S. Kumagai, H. Iguchi, S. Takaishi, B. K. Breedlove, M. Yamashita, H. Matsuzaki, H. Okamoto, K. Kato and M. Takata, *Inorg. Chem.*, 2014, **53**, 11764.